Catalysis Science & Technology

Accepted Manuscript

ROYAL SOCIETY OF CHEMISTRY

www.rsc.org/catalysis

Catalysis Science & Technology

Dynamic Article Links►

Cite this: DOI: 10.1039/c0xx00000x

Full Papers

www.rsc.org/xxxxxx

ZSM-5 seeds-grafted SBA-15 as a high performance support for cobalt Fischer-Tropsch Synthesis catalysts

Sufang Chen [a] *, Cunwen Wang[a] , Jinlin Li [b] **, Yuhua Zhang [b], Jingping Hong [b], Xiong Wen [b], Chengchao Liu [c]

Received (in XXX, XXX) Xth XXXXXXXXX 20XX, Accepted Xth XXXXXXXXX 20XX
DOI: 10.1039/b000000x

Abstract: A novel composite material ZSM-5/SBA-15 (SZM) was synthesized by grafting ZSM-5 zeolite seeds with mesoporous SBA-15 silica. This composite was used as Co (20 wt.%) catalyst support for Fischer–Tropsch Synthesis (FTS). The catalytic activity and product selectivity were significantly influenced by the content of ZSM-5 seeds. The 20Co/SZM-1 catalyst with lower content of ZSM-5 seeds showed the highest CO conversion (64.7%) as well as highest C_{5+} selectivity (83.6%).The 20Co/SZM-2 catalystwith higher content of ZSM-5 seeds exhibited the better bifunctional catalytic performance at higher reaction temperature (260°C).

Keywords: Fischer-Tropsch synthesis • cobalt catalyst • zeolite seeds • mesoporous aluminosilicate

1. Introduction

Fischer-Tropsch synthesis (FTS) is an important technology for the transformation of synthesis gas (syngas, CO and H_2 obtained from natural gas, coal or biomass) into ultra clean liquid fuels such as gasoline and diesel oil [1]. The products of FTS follow the Anderson–Schultz–Flory (ASF) polymerization model, with a wide range of straight-chain hydrocarbons and low selectivity of isomers [2]. For industry to selectively synthesize a specific type of product is still one of the most important challenges in FTS.

Many efforts have been dedicated to investigate the combination of acid catalysts with a conventional FTS catalyst to form a bifunctional catalyst system, in order to increase the product selectivity to a specific range[3-6]. In traditional system, hydrocracking catalysts (acidic zeolites) are usually packed in a separate reactor downstream or a separate layer below the FTS catalyst [7]. However, these two-section systems require additional equipment and much higher energy consumption. Thus, combination of FTS catalysts and hydrocracking catalysts in one-section generates increasing research interests [8]. Challenges are concentrated on the restricted access of reactants to the zeolite active sites, the diffusion limitation of products by small pores in ZSM-5, and high reaction temperatures, which led to lower catalyst activity and lifetime [9]. Mesoporous zeolite supported cobalt catalysts exhibited higher FTS activity and bifunctional properties[10], attributing to the structure of mesoporous hierarchy, which improved the Co dispersion and enhanced Co accessibility to active acid sites. Compared with mesoporous zeolite, ordered mesoporous aluminosilicates have tunable mesopores, higher specific surface area and larger pore volume, which could bring about an improved accessibility of reagent molecules to the active sites, and result in a facile transport of heavy hydrocarbons formed during FTS reaction [11]. However, these mesoporous aluminosilicate materials have relatively low acidity and low hydrothermal stability owing to the non-crystalline nature of the mesoporous walls, which severely limited their practical use [9].

Many efforts have been dedicated to maintain ordered mesoporous structure of aluminosilicate assembling from zeolite seeds with improved acidity and hydrothermal stability [12-14].The approach is based on surfactant directed assembly of zeolite seeds containing zeolite building units that normally nucleate in the early stage during zeolites synthesis[15]. The most significant advantage of this method is that the Al species in the mesostructure are mostly located at zeolite-like sites, which exhibited strong acidic sites in the products[14]. Therefore, the direct introduction of zeolite seeds into ordered mesoporous aluminosilicate takes advantages of both mesoporous materials (larger pores and good mass transfer) and zeolites (strong acidity

and good hydrothermal stability) [16].

In our earlier work, aluminum was introduced into the framework of SBA-16 [17] or SBA-15 [18], in order to change the product selectivity towards liquid hydrocarbons. However, the deactivation of these catalysts was quite significant [19]. Thus, in order to achieve high activity and long lifetime for further practical application, ordered mesoporous aluminosilicates assembled by ZSM-5 seeds (SZM) were used as supports of Co (20 wt.%) catalysts, and their catalytic performance in FTS was studied at different reaction temperature in this work. On the one hand, the zeolite seeds improve the acidity and hydrothermal stability of supports; on the other hand, their high surface area improves cobalt dispersion at elevated metal loadings. Insights into the catalytic performance of these bifunctional catalysts would enable us to fine-tune their product selectivity, and make these catalysts attractive for practical applications.

2. Experimental Section

2.1 Catalyst preparation

Ordered mesoporous aluminosilicate SZM-1 (Al/Si=0.015) assembled by ZSM-5 seeds was prepared according to the reported literature [14]. The detailed synthetic route was as follows: (1) The ZSM-5 seeds solution was prepared by adding 0.12 g of $NaAlO_2$, 6.0 g of tetraethylorthosilicate (TEOS) into 6.0 g of tetrapropylammonium hydroxide (TPAOH) aqueous solution (25%) with 12 g of H_2O. The mixture was stirred for 3 h at 40°C and then transferred into a closed Teflon bottle to age for 3 h at 100°C, to obtain a ZSM-5 seeds solution. (2) 0.8 g of $EO_{20}PO_{70}EO_{20}$ (Pluronic P123) was dissolved in 20.0 g of H_2O with 5 mL of HCl (10 mol L^{-1}) and stirred for 2 h at 40 °C to obtain a clear solution. Then, 3.8 g of TEOS and 7.0 g of ZSM-5 seeds solution were mixed with the P123 solution. The mixture was stirred for 24 h at 40 °C and then transferred into an autoclave for further reaction at 100 °C for 48 h. The precipitated material was filtered, washed with deionized water, dried at 110 °C for 10 h and calcined at 550 °C in air for 6 h (1 °C min^{-1}) to remove the templates. Another ordered mesoporous aluminosilicate SZM-2 (Al/Si=0.03) was prepared under the same synthesis conditions as the SZM-1 sample, except that instead of 7.0 g of ZSM-5 seeds solution, 21 g of ZSM-5 seeds solution was used. The Al/Si ratios of SZM products were calculated by ICP-AES. For comparison, SBA-15 material was also synthesized, following the procedures reported in literature [20].

The cobalt (20 wt.%) based catalysts were prepared by the conventional incipient wetness impregnation method, using cobalt nitrate as precursor of cobalt, and the SBA-15, SZM-1 and SZM-2 as supports. The impregnated catalysts were subsequently dried in a rotary evaporator from 50 °C to 90 °C, dried at 110 °C for 10 h, and then calcined at 350 °C for 5 h (2 °C min^{-1}). The corresponding FTS catalysts were denoted as 20Co/SBA-15, 20Co/SZM-1 and 20Co/SZM-2.

2.2 Catalyst characterization

ICP-AES analysis was performed on a Varian Liberty 200 vacuum unit inductively coupled plasma emission spectrometer to determine the Al/Si atomic ratios of supports. Nitrogen adsorption-desorption experiments were conducted at -196°C, with a Quantachrome Autosorb-1-C-MS. X-ray diffraction (XRD) patterns were obtained using a Bruker-D8 powder X-ray diffractometer. Transmission electron microscopy (TEM) images of the samples were obtained on a FEI Tecnai G^2 20 S-Twin microscope. Hydrogen temperature programmed reduction (H_2-TPR), hydrogen temperatures programmed desorption (H_2-TPD) and O_2 titration were carried out in a U-tube quartz reactor with a Zeton Altamira AMI-200 unit. The surface composition of the catalysts were determined from X-ray photoelectron spectroscopy (XPS), performed by a Vacuum Generator Mutilab 2000 spectrometer with a monochromatized Al K source (1486.6 eV). The temperature-programmed desorption of ammonia (NH_3-TPD) was conducted on a Finesorb-3010 instrument.

2.3 Fischer-Tropsch synthesis (FTS)

FTS reactions were conducted in a fixed bed reactor (id = 12 mm), and typically, the catalyst (0.5 g) was mixed with carborundum (5.0 g). Prior to the reaction, the catalyst was reduced at 450°C for 10 h in a flow of high purity H_2 with a space velocity of 6000 mL g_{cat}^{-1} h^{-1}. After reduction, syngas (H_2/CO = 2) was fed into the reactor after the catalyst was cooled down to 100 °C. The FTS reaction was carried out subsequently under the following reaction conditions: T = 220 °C, P = 1.0 MPa and GHSV = 6000 mL g_{cat}^{-1} h^{-1}. The wax and water products were collected in a hot trap (100 °C), and the oil and water products in a cold trap (-2 °C). The outlet gas was analyzed online using an Agilent 3000A Micro GC. The oil and wax products were analyzed with an Agilent 6890N GC and an Agilent 7890A GC, respectively.

3. Results and Discussion

The ICP-AES results are listed in Table 1. The Al/Si ratios of SZM-1 and SZM-2 samples are 0.0014 and 0.0022, respectively, these values are much lower than those in the initial reaction gels (0.015 and 0.030), suggesting that most of Al species were washed away during the synthesis process.The cobalt content of the three catalysts are quite close to the nominal value of 20 wt.%, indicated that almost all cobalt species were introduced into the final products through incipient wetness impregnation method.

Table 1. Textural parameters of samples

Samples	Al/Si [a]	Co (wt.%)[a]	S_{BET} (m^2g^{-1}) [b]	V_{total} (cm^3g^{-1})	D (nm) [c]
SBA-15	0		814.5	1.53	7.4
SZM-1	0.0014		724.4	1.37	7.0
SZM-2	0.0022		739.2	1.13	6.5
20Co/SBA-15	-	19.89	466.1	0.854	6.9
20Co/SZM-1	-	20.13	372.4	0.693	6.9
20Co/SZM-2	-	20.08	370.3	0.559	6.4

[a] Calculated by ICP-AES, [b] Calculated by the BET method, [c] Average pore diameter.

The porous properties of the supports and the catalysts were examined by N_2 adsorption-desorption isotherms at -196°C. The textural and structural properties are summarized in Table 1.

Compared with SBA-15, the BET surface areas, total pore volume, and the pore diameter of ordered mesoporous aluminosilicate material assembled by ZSM-5 seeds (SZM-1 and SZM-2) all decreased (Table 1), attributing to the presence of larger micropore volume than SBA-15[15]. After cobalt impregnation, the pore diameter, surface area and total pore volume of the catalysts were further decreased, attributing to the deposition of the Co_3O_4 species on the support pore walls.

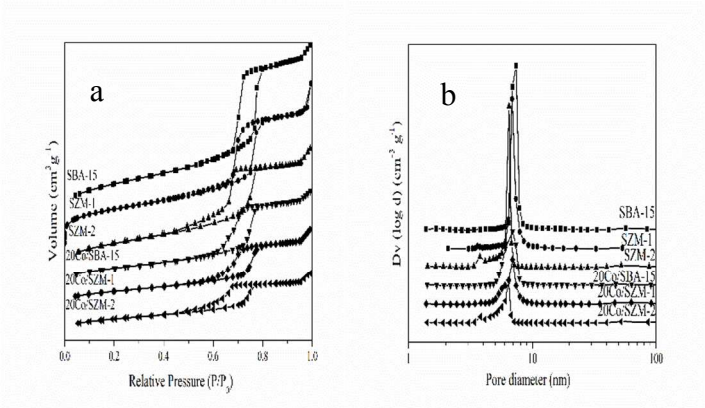

Figure 1 (a) N_2 adsorption–desorption isotherms of supports and catalysts and (b) BJH pore size distribution curves of supports and catalysts.

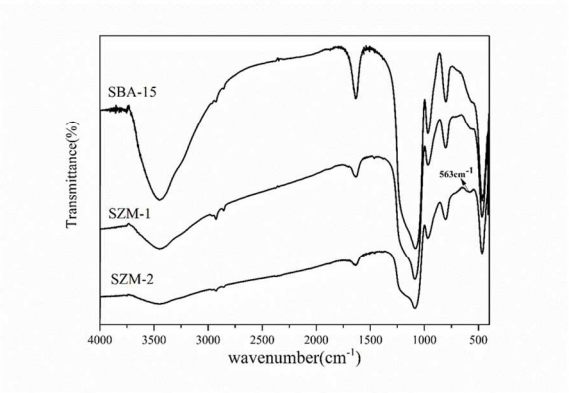

Figure 2 IR spectra of three supports

N_2 adsorption–desorption isotherms of both the supports and the corresponding catalysts are displayed in Figure 1a. All samples exhibit typical type IV isotherms with H1-type hysteresis loops and a sharp capillary step in the P/P_0 range of 0.6-0.8, which are characteristic of ordered mesoporous material with cylindrical pore geometry, similar to the mesoporous structure of SBA-15 [21]. No change in the type of isotherm and the shape of the hysteresis loop is observed between the supports and their corresponding supported catalysts. This indicates that the pore structure in the support is preserved after the deposition of cobalt. The height of the hysteresis loop decreases after cobalt loading due to the blocking of mesopores by cobalt deposition.

The BJH pore size distributions of supports and catalysts are showed in Figure 1b. All samples exhibit a narrow pore size distribution, and SBA-15 support has the largest BJH pore size of 7.4 nm, in agreement with the data listed in Table 1. The SZM-2 support possesses a major BJH pore size distribution at 5.9 nm and a weak one at around 4 nm, this is probably due to the stability of the mesoporous walls that are formed by assembling the ZSM-5 seeds primary units and its lower tendency toward shrinkage during the decomposition of the template [22].

IR spectra of three supports (Figure 2) show similar bands in the region of 1000-4000 cm^{-1}. However, an additional band at 563 cm^{-1}, which are similar to those of the five-membered rings of T-O-T (T = Si or Al) in zeolite crystals[14], becomes stronger with further increasing content of ZSM-5 seeds. These results indicate that the mesoporous walls of SZM contain the primary units of ZSM-5.

TEM images of the SZM materials with different ZSM-5 seeds content (Figure 3) show highly ordered 2-D hexagonal mesostructures, and their pores (~7nm) are clearly visible in the TEM images. These observations are well in agreement with the results of N_2 adsorption-desorption, which indicate that ZSM-5 seeds assembled aluminosilicates have uniform tubular pore channels, similar to ordered mesoporous siliceous SBA-15.

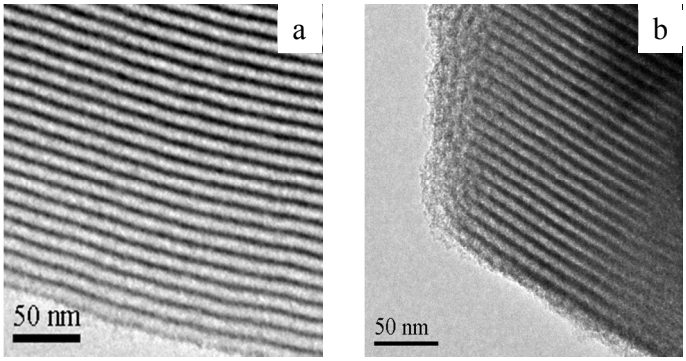

Figure 3 TEM images of（a）SZM-1 and（b）SZM-2

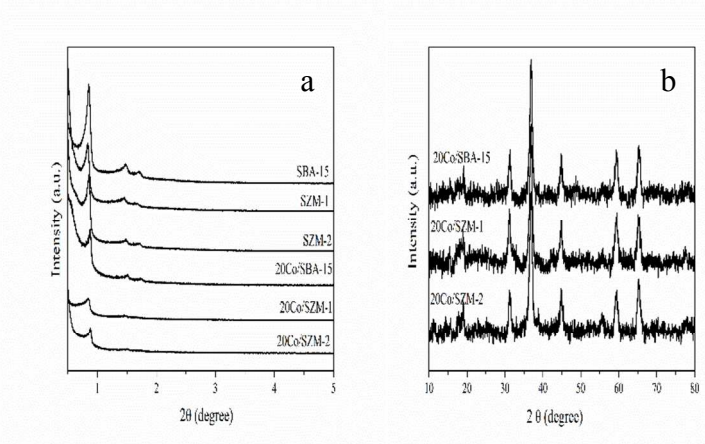

Figure 4 (a) Small-angle XRD patterns of supports and catalysts; (b) Large-angle XRD patterns of catalysts

Figure 4a shows the small-angle powder XRD patterns of the samples. All the samples show three well resolved peaks which are indexed to the (100), (110) and (200) reflections of the well-ordered two-dimensional (2D) hexagonal structure with *p6mm* symmetry, which are typical of SBA-15 mesoporous structure [23], consistent with the results of TEM and nitrogen

sorption isotherms. After cobalt impregnation, the intensity of the (100), (110) and (200) diffraction lines are weaker than the corresponding supports, due to the deposition the Co_3O_4 crystalline on the support pore walls. Large-angle powder XRD patterns of the three catalysts are shown in Figure 4b. All Co catalysts show the characteristic reflection peak of Co_3O_4 phase at $2\theta = 36.8°$ [24]. The particle sizes of Co_3O_4 crystallites, calculated by the Scherrer equation, are 11.5, 11.9 and 10.7 nm for 20Co/SBA-15, 20Co/SZM-1 and 20Co/SZM-2 respectively.

The reducibility of the three catalysts was measured by H_2-TPR experiments and the reduction patterns are displayed in Figure 5. Three major peaks are observed at different temperature regions, i.e., a relatively sharp peak below 350 °C, broad peaks between 350 °C to 550 °C, and peaks above 550 °C. The first peak is assigned to the reduction of Co_3O_4 to CoO, and the second region peaks between 350°C and 550 °C are attributed to the reduction of CoO to metallic cobalt, the third region peaks above 550 °C correspond to the reduction of barely reducible cobalt oxide species [25]. Comparing with 20Co/SBA-15 and 20Co/SZM-2 catalysts, the second region reduction peaks in 20Co/SZM-1 catalyst shift to lower temperatures with increasing peak intensity, indicating higher reducibility of cobalt species on the 20Co/SZM-1 catalyst, which is due to the larger particle size of Co_3O_4 crystallites.

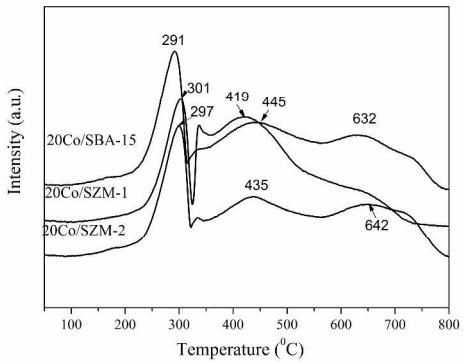

Figure 5 H_2-TPR profiles of the three catalysts

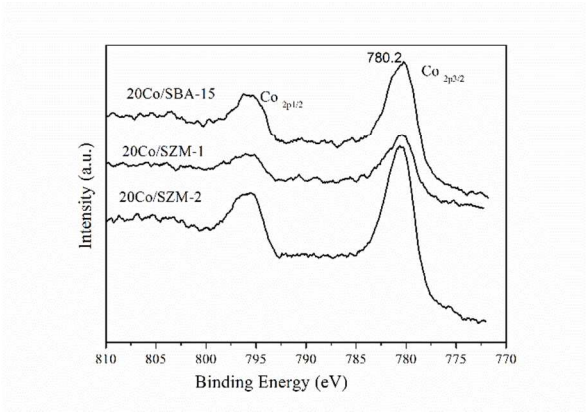

Figure 6 XPS spectra of catalysts

Surface compositions of the catalysts are investigated by X-ray photoelectron spectroscopy (XPS) and the results are shown in Figure 6. The Co 2p profiles of the catalysts display the characteristic doublet corresponding to the spin–orbit coupling ($2p_{3/2}$, $2p_{1/2}$) with the most intense $Co_{2p3/2}$ peak at binding energies 780.1–780.4 eV[24], which suggests that the main phase on the catalysts surface is Co_3O_4 [26], in agreement with the XRD results. To investigate the changes in the surface composition after the addition of ZSM-5 seeds, the atomic ratio of Co/Si is calculated and the obtained quantitative results are displayed in Table 2. The lowest atomic ratio of Co/Si ratio is observed on 20Co/SZM-1 catalyst, indicating lower dispersion of Co species at the catalyst surface than the other two catalysts (20Co/SBA-15 and 20Co/SZM-2) [8],in agreement with the data of H_2-TPD results.

The dispersion and reducibility of the three catalysts were measured the hydrogen temperature-programmed desorption (H_2-TPD) and O_2 titration and the data are present in Table 2. The 20Co/SZM-1 catalyst shows the lowest dispersion with largest cobalt particles among the three catalysts, consistent with the XPS results. After reduction in H_2 flow at 450 °C for 10 h, the reduction degree of 20Co/SBA-15, 20Co/SZM-1 and 20Co/SZM-2 catalysts are 68.6%, 71.2% and 63.3%, respectively, the 20Co/SZM-1 catalyst shows the highest cobalt reducibility, consistent with the TPR results. The cobalt particle sizes calculated by H_2-TPD and O_2 titration are 8.8, 9.7 and 5.8 nm for 20Co/SBA-15, 20Co/SZM-1 and 20Co/SZM-2 respectively (Table 2). Total acidity amount of the three catalysts are also showed in Table 2. The content of acidity increased with increasing ZSM-5 content in catalysts.

Table 2 XPS, H_2-TPD and O_2-titration data of the three catalysts

Catalysts	Co/Si [a]	d_{Co} (nm) [b]	D (%) [c]	R (%) [d]	Acidity (μmol g-1) [e]
20Co/SBA-15	0.029	8.8	10.9	68.6	1.7
20Co/SZM-1	0.024	9.7	9.9	71.2	18.6
20Co/SZM-2	0.052	5.8	16.5	63.3	25.7

[a]Atomic ratio calculated from XPS; [b] Cobalt particle size calculated by H_2-TPD and O_2 titration; [c] Catalyst dispersion calculated by$D=96/d_{Co}$; [d] Catalyst reducibility ; [e] Total acidity amount calculated from NH_3-TPD.

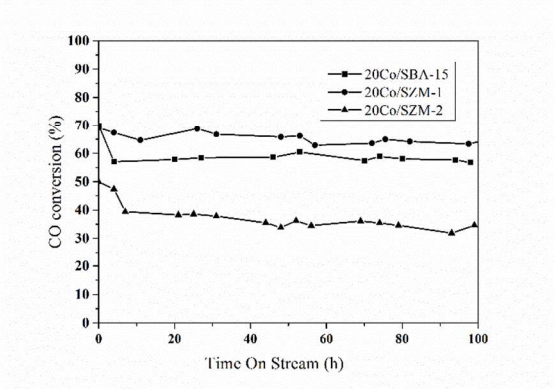

Figure 7 Catalytic activities of the catalysts with time on stream.

Figure 7 shows the evolution of FTS activity of the three catalysts with time on stream. Steady state was generally reached after 20 h TOS for all catalysts.The data of FTS activity and product selectivity for the catalysts under steady state are listed in Table 3.The turnover frequency (TOF) for CO conversion is 11.3, 11.5 and $4.7x10^{-3}$ s^{-1} for 20Co/SBA-15, 20Co/SZM-1 and Co/SZM-2 respectively (Table 3). The results reveal that the TOF of 20Co/SBA-15 and 20Co/SZM-1 was independent of cobalt particle size for catalysts with sizes larger than 6 nm[25]. The lower TOF of 20Co/SZM-2 is attributed to the cobalt particle sizes (5.8nm) below the "critical" size of 8-10 nm for which a TOF-particle size dependence has been previously reported[27, 28]. The CO conversion of 20Co/SZM-1 (64.7 %) is higher than that of 20Co/SBA-15 catalyst (58.6%),which is due to the higher cobalt reducibility in 20Co/SZM-1 catalyst with the similar TOF for CO conversion[29]. However, with further increase of ZSM-5 seeds content, a decrease of CO conversion is observed on the 20Co/SZM-2 catalyst (35.4%) due to the lower TOF for CO conversion.

Table 3 The FTS activity and selectivity of three catalysts

Catalysts	CO (%)[a]	TOF (s-1) [b]	CH_4 (%)	C_2-C_4 (%)	C_{5+} (%)
20Co/SBA-15	58.6	11.3	11.8	10.1	78.1
20Co/SZM-1	64.7	11.5	8.4	8.0	83.6
20Co/SZM-2	35.4	4.7	17.0	12.2	70.8
20Co/SZM-2[c]	65.2	6.1	12.6	8.8	78.6

[a] Reaction conditions: 1.0 MPa, H_2/CO = 2:1, 220 °C, 6000 mL $g^{-1}h^{-1}$, FTS data were collected at a steady state (80 h);[b] TOF=10^{-3} s^{-1} based on dispersion H_2 chemisorption. [c] Reaction conditions: 1.0 MPa, H_2/CO = 2:1, 220 °C, 4000 mL $g^{-1}h^{-1}$;

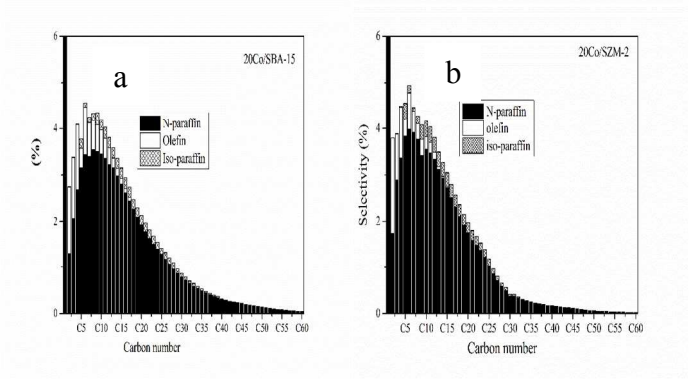

Figure 8 Distribution of hydrocarbons on (a) 20Co/SBA-15 and (b) 20Co/SZM-2

The product selectivities are also shown in Table 3, the 20Co/SZM-1 catalyst exhibits a highest selectivity of C_{5+} heavy hydrocarbons (83.6%) and lowest selectivity of CH_4 (8.4%), while the 20Co/SZM-2 catalyst shows a lowest selectivity of C_{5+} heavy hydrocarbons (70.8%) and highest selectivity of CH_4 (17.0%). The high CH_4 selectivity observed on 20Co/SZM-2 (Table 3) could be well due to its much lower CO conversion. When decreasing the gas velocity to achieve the CO conversion at similar level with other two catalysts, 20Co/SZM-2 catalyst shows a comparable CH_4 selectivity, as shown in Table 3. In addition, lower Co particle sizes of 20Co/SZM-2 (5.8 nm) would also lead to higher methane selectivity and to lower C_{5+} selectivity. The results might also indicate a lower abundance of sites active for chain growth, resulting in more carbon species at the surface that become fully hydrogenated to methane[30].

Distribution of hydrocarbon products on the 20Co/SBA-15 and 20Co/SZM-2 catalysts with ZSM-5 seeds is shown in Figure 8. Comparing with 20Co/SBA-15 catalyst, the formation of hydrocarbons with carbon number > 30 is significantly reduced and the fraction of iso-paraffins is remarkably increased over 20Co/SZM-2 catalyst, which could be due to the increasing concentration of effective acid sites, confirmed by NH_3-TPD results (Table 2). As a result, the selectivity of heavy hydrocarbons decreased while the selectivity of iso-paraffins increased with increasing ZSM-5 seeds.

Table 4 The FTS performance of 20Co/SZM-2 and 20Co/SBA-15

Catalysts	CO (%)[a]	CH_4 (%)	C_2-C_4 (%)	C_5.C_{20} (%)	C_{20+} (%)	Iso/N (%)[b]	O/N (%)[c]
20Co/SBA-15	86.9	36.5	23.4	38.9	1.2	15.3	14.7
20Co/SZM-2	77.2	20.3	16.7	60.1	2.9	21.5	26.6

[a] Reaction conditions: 1.0 MPa, H_2/CO = 2:1, 260 °C, 8000 mL $g^{-1}h^{-1}$;
[b] Iso/N calculated from Iso-paraffins /N-paraffins*100% in the range of C_5–C_{20} hydrocarbons;
[c] O/N calculated from Olefin / N-paraffins*100% in the range of C_5–C_{20} hydrocarbons.

In order to better illustrate bifunctional catalytic performance, FTS reaction at the higher reaction temperature (260°C) was performed for20Co/SBA-15 and 20Co/SZM-2 catalysts, and the selectivity data are also presented in Table 4. Compared with the acid-free 20Co/SBA-15 catalyst, the 20Co/SZM-2 catalyst with higher acid content exhibits much lower selectivity of CH_4 (20.3%), higher selectivities of O/N (21.5%) and Iso/N (26.6%) in the range of C_5-C_{20} hydrocarbons. The strong acidic catalyst favors the formation of isomers in the range of C_5-C_{20} hydrocarbons at the expense of C_{20+} hydrocarbons [31].The reduced heavy hydrocarbons selectivity with increasing selectivities of olefin and iso-paraffins is correlated with the higher reaction temperature, which increases the cracking properties of heavy products due to the presence of acidic sites on the supported catalysts[8].

4. Conclusions

Ordered mesoporous aluminosilicate materials (SZM-1 and SZM-2) assembled by ZSM-5 seeds with high surface area, pore volume and proper mesoporous structure have been successfully synthesized. The content of ZSM-5 seeds for cobalt-based catalyst has significant impact on the catalytic activity as well as heavy hydrocarbons selectivity, olefin selectivity and iso-paraffins selectivity during the FTS reaction. The 20Co/SZM-1 catalyst with lower ZSM-5 seeds content shows higher CO conversion (64.7%) with good stability, as well as higher C_{5+} selectively (83.6%) and lower CH_4 selectivity (8.4%). Increasing reaction temperature leads to a better bifunctional performance, the 20Co/SZM-2 catalyst reacted at 260°C shows high O/N selectivity (26.6%) and high Iso/N selectivity (21.5%) in the range of C_5-C_{20} hydrocarbonsin FTS.

Acknowledgements

This work was supported by National Natural Science foundation of China (21403158, 21473259 and 21203255), Key Program project of the NSFC and China Petrochemical Corporation Joint Fund, U1463210, Scientists Foundation of Wuhan Institute of Technology (K201443), and the Hubei Province Key Laboratory of Coal Conversion and New Carbon Materials (WKDM201304).

Notes and references

*[a] *Key Laboratory for Green Chemical Process of Ministry of Education, Hubei Key Laboratory of Novel Reactor and Green Chemical Technology, School of Chemical Engineering and Pharmacy, Wuhan Institute of Technology, Wuhan, Hubei 430073, China P.R. E-mail: csfzdh@126.com*

*[b]*Key Laboratory of Catalysis and Materials Science of the State Ethnic Affairs Commission & Ministry of Education, South-central University for Nationalities, Wuhan, Hubei 430073, China P.R. Fax:+86 27 67842752. E-mail: jinlinli@aliyun.com*

[c]The Hubei Province Key Laboratory of Coal Conversion and New Carbon Materials, School of Chemical Engineering and Technology, Wuhan University of Science and Technology, Wuhan, Hubei 430081, China P.R.

1. F. Fischer and H. Tropsch, *Brennstoff-Chem*, 1923, 4, 276-285.
2. B. Shi and B. H. Davis, *Appl. Catal., A*, 2004, 277, 61-69.
3. X. Li, M. Luo and K. Asami, *Catal. Today*, 2004, 89, 439-446.
4. K. Cheng, J. C. Kang, S. W. Huang, Z. Y. You, Q. H. Zhang, J. S. Ding, W. Q. Hua, Y. C. Lou, W. P. Deng and Y. Wang, *ACS Catal.*, 2012, 2, 441-449.
5. J. C. Kang, K. Cheng, L. Zhang, Q. H. Zhang, J. S. Ding, W. Q. Hua, Y. C. Lou, Q. G. Zhai and Y. Wang, *Angew. Chem. Int. Ed.*, 2011, 123, 1-5.
6. Q. H. Zhang, J. C. Kang and Y. Wang, *ChemCatChem*, 2010, 2, 1030 -1058.
7. Z. W. Liu, X. H. Li, K. J. Asami and K. Fujimoto, *Appl. Catal., A*, 2006, 300, 162-169.
8. S. H. Kang, J. H. Ryu, J. H. Kim, P. S. Prasad, J. W. Bae, J. Y. Cheon and K. W. Jun, *Catal. Lett.*, 2011, 141, 1464-1471.
9. X. Vu, U. Bentrup, M. Hunger, R. Kraehnert, U. Armbruster and A. Martin, *J Mater Sci*, 2014, 49, 5676-5689.
10. S. Sartipi, M. Alberts, V. P. Santos, M. Nasalevich, J. Gascon and F. Kapteijn, *ChemCatChem*, 2014, 6, 142-151.
11. S. Chen, J. Li, Y. Zhang, Y. Zhao and J. Hong, *Catal. Sci. Technol.*, 2013, 1063-1068.
12. Y. Liu and T. J. Pinnavaia, *Chem. Mater.*, 2002, 14, 3-5.
13. Y. Liu and T. J. Pinnavaia, *J. Mater. Chem.*, 2002, 12, 3179-3190.
14. Y. Han, S. Wu, Y. Sun, D. Li, F.-S. Xiao, J. Liu and X. Zhang, *Chem. Mater.*, 2002, 14, 1144-1148.
15. F. Chen, X. Meng and F.-S. Xiao, *Catal. Surv. Asia*, 2011, 15, 37-48.
16. K. Cho, K. Na, J. Kim, O. Terasaki and R. Ryoo, *Chem. Mater.*, 2012, 24, 2733-2738.
17. Y. Zhao, J. Li, Y. Zhang, S. Chen and K. Liew, *ChemCatChem*, 2012, 4, 1926-1929.
18. S. Chen, J. Li, Y. Zhang, Y. Zhao, K. Liew and J. Hong, *Catal. Sci. Technol.*, 2014, 4, 1005-1011.
19. P. Munnik, P. E. de Jongh and K. P. de Jong, *J. Am. Chem. Soci.*, 2014, 136, 7333-7340.
20. D. Y. Zhao, J. L. Feng, Q. S. Huo, N. Melosh, G. H. Fredrickson, B. F. Chmelka and G. D. Stucky, *Science*, 1998, 279, 548-552.
21. A. Taguchi and F. Schüth, *Microporous Mesoporous Mater.*, 2005, 77, 1-45.
22. D. Zhang, A. Duan, Z. Zhao and C. Xu, *J. Catal.*, 2010, 274, 273-286.
23. Q. Li, Z. Wu, B. Tu, S. S. Park, C.-S. Ha and D. Zhao, *Microporous Mesoporous Mater.*, 2010, 135, 95-104.
24. A. Pereira, J. González-Carballo, F. Pérez-Alonso, S. Rojas, J. Fierro and M. d. Rangel, *Top. Catal.*, 2011, 54, 179-189.
25. M. Lualdi, G. Di Carlo, S. Lögdberg, S. Järås, M. Boutonnet, V. La Parola, L. F. Liotta, G. M. Ingo and A. M. Venezia, *Appl. Catal., A*, 2012, 443–444, 76-86.
26. S. J. Park, S. M. Kim, M. H. Woo, J. W. Bae, K. W. Jun and K. S. Ha, *Appl. Catal., A*, 2012, 419–420, 148-155.
27. G. L. Bezemer, J. H. Bitter, H. P. C. E. Kuipers, H. Oosterbeek, J. E. Holewijn, X. Xu, F. Kapteijn, A. J. van Dillen and K. P. de Jong, *J. Am. Chem. Soci.*, 2006, 128, 3956-3964.
28. A. Martínez, G. Prieto and J. Rollán, *J. Catal.*, 2009, 263, 292-305.
29. S. Bessell, *Appl. Catal., A*, 1993, 96, 253-268.
30. E. Iglesia, *Appl. Catal., A*, 1997, 161, 59-78.
31. R. Oukaci, J. C. S. Wu and J. G. Goodwin Jr, *J. Catal.*, 1988, 110, 47-57.